ELSEVIER

Journal of Hazardous Materials B118 (2005) 227–237

Journal of Hazardous Materials

www.elsevier.com/locate/jhazmat

Model applications and mechanism study on the degradation of atrazine by Fenton's system

K.H. Chan, W. Chu*

Department of Civil and Structural Engineering, Research Centre for Environmental Technology and Management, The Hong Kong Polytechnic University, Hung Hom, Kowloon, Hong Kong

Received 15 September 2004; received in revised form 11 November 2004; accepted 13 November 2004
Available online 19 December 2004

Abstract

Atrazine (ATZ), 2-chloro-4-(ethylamino)-6-(isopropylamino)-*s*-triazine, was effectively degraded by hydroxyl radicals that were generated by Fe^{II}/H_2O_2 in the Fenton's process. Up to 98% ATZ removal can be achieved in the process if the doses of Fe^{II} and H_2O_2 are selected appropriately. Oxidation capacity of the process was successfully predicted through a kinetic approach with three simple and measurable parameters (i.e., two rate constants and a break point time), which makes the model useful in predicting, controlling and optimizing the degradation of ATZ. In addition, the transformation pathways of ATZ decay was successfully investigated by using a novel technology, liquid chromatography electrospray tandem mass spectrometry (LC/ESI-MS/MS). Ten intermediates were identified in the process. The alkylic-oxidation followed by dealkylation and/or dechlorination–hydroxylation were found to be the major pathways of the decay of ATZ in Fenton's process. All the detected intermediates were found to be dealkylated in different levels or positions. The dealkylated species may be further dechlorinated but generally at a lower fraction (<10%) due to the depletion of oxidants.

Keywords: Atrazine; Catalyzed oxidation; Ferrous; Fenton; Hydrogen peroxide; Intermediates; Model

1. Introduction

The herbicide atrazine (ATZ) is routinely used in combating weeds in corn and sorghum crops, and is also widely used in combination with other herbicides. It is a pollutant that causes environmental concern because of its low biodegradability. It has a high potential to contaminate surface waters and groundwater. Recently, the impact of ATZ on endocrine disruption is very serious. ATZ affects hormone metabolism in women, which may have possible implications for breast cancer [1]. ATZ belongs to the group of symmetric triazine derivatives. Its solubility in water is low ($33\,\mu g\,mL^{-1}$ at 22 °C) and independent to pH [2]. Besides, ATZ is less reactive (round 200–1000 times) to photosynthesis than its transformation products such as diaminochlorotriazine and hydroxylatrazine [3]. These transformation products are generally less toxic to aquatic plants. Eisler [4] concluded that "there is a general agreement that atrazine degradation products were substantially less toxic than the parent compound and not normally present in the environment at concentrations inhibitory to algae, bacteria, plants, or animals."

Fenton's process used in this study is a technology of using ferrous-catalyzed hydrogen peroxide to provide an oxidizing environment at acidic pH. The process has been used in both the oxidative treatment of industrial effluents and in the manufacture of several types of polymers and polyelectrolytes. The use of Fenton's reagent to remove less-biodegradable organics in wastewater is relatively new compared to its use in mechanistic investigations in organic chemistry. It is attractive due to the fact that iron is an abundant and non-toxic element, and because hydrogen peroxide is easy to handle and can be broken down to environmentally benign products. The Fenton's process is able to destroy phenols, chlorinated phenols and herbicides in water media, as well as reduce chemical oxygen demand in municipal waste [5].

* Corresponding author. Tel.: +852 2766 6075; fax: +852 2334 6389.
E-mail address: cewchu@polyu.edu.hk (W. Chu).

0304-3894/$ – see front matter © 2004 Elsevier B.V. All rights reserved.
doi:10.1016/j.jhazmat.2004.11.008

Nomenclature

[ATZ]	concentration of atrazine (mmol L^{-1})
$[ATZ]_0$	concentration of atrazine at the beginning of reaction (mmol L^{-1})
$[ATZ]_b$	concentration of atrazine at the break point of the two phases (mmol L^{-1})
b_1	rate constant in phase I (mmol L^{-1} s^{-1})
b_2	rate constant in phase II (mmol L^{-1} s^{-1})
CAAT	2-chloro-4,6-diamino-*s*-triazine
CDAT	2-chloro-4-acetamido-6-amino-*s*-triazine
CDET	2-chloro-4-acetamido-6-(ethylamino)-*s*-triazine
CDIT	2-chloro-4-acetamindo-6-(isopropylamino)-*s*-triazine
CEAT	2-chloro-4-(ethylamino)-6-amino-*s*-triazine
CIAT	2-chloro-4-(isopropylamino)-6-amino-*s*-triazine
CMIT	2-chloro-4-(1-methylethanolamino)-6-(isopropylamino)-*s*-triazine
DDW	distilled–deionized water
ESI-MS/MS	electrospray-ionization tandem-mass-spectrometry
F/H ratios	Fe^{II} to H_2O_2 ratios
[Fe(II)]	concentration of ferrous ion (mmol L^{-1})
HPLC	high-pressure-liquid-chromatography
$[H_2O_2]$	concentration of hydrogen peroxide (mmol L^{-1})
I_b	the *y*-intercept of the plot of ln b_1 against ln b_2
I_r	the *y*-intercept of the plot of ln b_1 against F/H ratio
ID	internal diameter
met-CMIT	2-chloro-4-(1-carboxylethanolamino)-6-(isopropylamino)-*s*-triazine
$[M+H^+]$	positive ions
OAAT	ammeline, 2-hydroxy-*o*-4,6-diamino-*s*-triazine
ODAT	2-hydroxy-4-acetamido-6-amino-*s*-triazine
ODET	2-hydroxy-4-acetamido-6-(ethylamino)-*s*-triazine
ODIT	2-hydroxy-4-acetamindo-6-(isopropylamino)-*s*-triazine
OEAT	2-hydroxy-4-(ethylamino)-6-amino-*s*-triazine
OIAT	2-hydroxy-4-(isopropylamino)-6-amino-*s*-triazine
OIET	2-hydroxy-4-(isopropylamino)-6-(ethylamino)-*s*-triazine
t	reaction time (s)
t_b	break point time (s)
UV	ultra-violet

Hydrogen peroxide decomposes catalytically in the presence of ferrous ions and generates radicals such as the hydroxyl ($^{\bullet}OH$) and hydroperoxyl ($^{\bullet}OOH$) radicals. It has been shown that the hydroxyl radical is the major oxidizing species in this system, and is mainly formed according to the following reaction [6].

$$Fe^{2+} + H_2O_2 \rightarrow Fe^{3+} + OH^- + {}^{\bullet}OH$$

Nevertheless, the nature of these species is still under discussion and its formulation has been a subject of controversy in the past and recent Fenton's-related literature [7–11].

In our previous study, the initial concentrations of ferrous ion and the Fe^{II} to H_2O_2 ratios (F/H ratios) were reported as the dominant parameters that determined the efficiency of the Fenton's process [12]. In general, the use of higher doses or F/H ratios guarantees faster and more comprehensive removal of the target compound; however, unnecessary over-dosing or disregarded under-dosing make the process less cost-effective or non-efficient. Thus it is especially important to optimize such a treatment system by evaluating the necessary information of the kinetics data together with the doses of Fe^{II} and H_2O_2. Hence, the objective of the present work were: (i) to determine the capacity and/or performance of the ATZ oxidation through the examination of reaction kinetics at various dosages of hydrogen peroxide and ferrous ion; (ii) to propose the practical model based on these findings; (iii) to investigate the transformation products and to evaluate the degradation pathways of the ATZ decay in Fenton's process. The identification of reaction intermediates was performed using liquid chromatography (LC) together with the stae-of-the-art electrospray ionization-mass spectrometry (ESI-MS) and tandem mass spectrometry (MS/MS), which separate and directly characterize the reaction products to reveal the degradation mechanism and reaction pathways of the process.

2. Methodology

2.1. Chemicals

Nonlabeled ATZ at 99% purity and its main decayed intermediates (which were available in market) were purchased from RdH Laborchemikalien GmbH & Co. including 2-chloro-4-(isopropylamino)-6-amino-*s*-triazine, 99.9% (CIAT), 2-chloro-4-(ethylamino)-6-amino-*s*-triazine, 96.1% (CEAT), 2-hydroxy-4-(isopropylamino)-6-(ethylamino)-*s*-triazine, 94.7%(OIET), 2-hydroxy-4-(ethylamino)-6-amino-*s*-triazine, 95.4% (OEAT), and 2-hydroxy-4-(isopropylamino)-6-amino-*s*-triazine, 98.7% (OIAT). The stock solutions of ATZ, CIAT, CEAT, OIET, OEAT and OIAT were prepared in stock solution at 0.116, 0.128, 0.212, 0.05, 0.100 and 0.106 mmol L^{-1}, respectively, in HPLC-water. Acetonitrile (from Labscan Asia Co. Ltd.) was degassed before being used in high-performance liquid chromatography (HPLC). Ferrous salt ($FeSO_4{\cdot}7H_2O$) and

H_2O_2 (30% solution) were purchased from RbH and Junsei Chemical Ltd. (Japan), respectively. Sulfuric acid was used to adjust the pH of the system, and methanol purchased from Labscan was used as a quenching solution.

2.2. Test methods

A series of batch tests were employed to determine the degradation of ATZ under different Fe^{II} concentrations and F/H ratios. Various F/H ratios at 0.33, 0.50, 1.00, 2.00 and 3.00 were adjusted by different proportions of Fe^{II} and H_2O_2. The concentrations of Fe^{II} were adjusted at 0.05, 0.10, 0.15 and 0.20 mmol L^{-1}, and the solution pH in this study was set at 2 by using 4 M H_2SO_4 buffer solution. The reactors were enclosed by aluminum foil to prevent any side reaction from the light in the room. Samples of 1 mL taken at different treatment times were mixed with the same volume of methanol to quench the reaction [10]. The quenched solution was then centrifuged at 3200 rpm for 10 min, and the supernatant was filtered by 90 μm filter and analyzed by HPLC to quantify the remaining ATZ in the system.

2.3. Analytical methods

2.3.1. High-pressure-liquid-chromatography (HPLC)

For the investigation of ATZ degradation, the samples were collected from different reaction time and analyzed by HPLC. The HPLC, Finnigan SpectraSYSTEM® LC, comprised a solvent degasser, quaternary gradient pump, inert autosampler with a 20 μL injection loop, and photodiode array UV detector. The chromatographic separations were performed on the stainless steel Restek column: 5 μm 4.6 (i.d.) × 250 mm Pinnacle™ Octyl Amine column. The maximum absorption wavelength of ATZ was selected at 221 nm. The mobile phase consisted of 60% acetonitrile with 40% DDW was delivered at a flow rate of 1.5 mL min^{-1}, which resulted in an ATZ peak at 3.5 min. In addition, a five-point calibration curve was run for ATZ with detection limit of 1.59 μM.

2.3.2. Electrospray-ionization tandem-mass-spectrometry (ESI-MS/MS)

The investigation of ATZ's transformation intermediates were performed by HPLC cooperated with electrospray-ionization and tandem-mass-spectrometry (HPLC/ESI-MS/MS), Finnigan ThermoQuest LCQ Duo. The eluent (1 mL min^{-1}) was delivered by a gradient system from HPLC and partitioned by an Alltech (Alltech Associates Inc.) Hypersil ODS column (C_{18}, 5 μm, 4.6 × 250 mm). The elution was carried out with a gradient flow of from 95 to 0% of ammonia acetate (5 mmol L^{-1}, pH 4.6), and from 5 to 89% of acetonitrile, together with 0–11% of water in 15 min. After the analytical run, the column was rinsed with a solution containing 50% methanol and 50% water for 5 min and the mobile phase returned to the initial condition in 5 min. The maximum absorption wavelength of ATZ and its transformation intermediates were ranged in 207–221 nm. Four-point calibration curves were run for ATZ and its transformation products. When the standards were not available, the response factors were adapted from compounds of a similar nature (chloro- or hydroxyl-triazines as determined by the UV spectra) and from the retention times. The LC eluent was then directed to the ESI, and positive ions ($M + H^+$) were detected in the selected reaction monitoring mode. The ESI probe was installed with sheath and auxiliary gasses run at 80 and 20 units, respectively. MS conditions were as follows: the capillary temperature was set at 250 °C with a voltage of 46 V and a spray voltage of 4.5 kV. The MS/MS experiments were carried out by using helium as the collision gas (30, 100% collision energy corresponding to 5 V from peak to peak).

Table 1
Identified degradation products and their main fragments determined by LC/ESI-MS/MS

Compounds	Retention time (min)	$[M + H^+]$	ESI-MS/MS spectrum (m/z) ions
ATZ	12.43	216	216, 174, 146, 132, 110, 104, 96, 68
met-CMIT	11.92	246	246, 188, 130, 104
CDIT	9.77	230	230, 188, 146, 110, 104, 79, 68
CIAT	8.80	188	188, 146, 110, 104, 79, 68
OIET	8.20	198	198, 156, 128, 114, 86
CEAT	7.45	174	174, 146, 132, 110, 104, 96, 79, 68
CDET	7.38	216	216, 188, 174, 146, 132, 104, 96, 79, 71, 68
OAAT	6.25	128	128, 86
ODIT	6.02	212	212, 170, 128, 86
ODET	6.00	198	198, 170, 156, 128
CDAT	5.60	188	188, 146
ODAT	5.55	170	170, 128, 86
OIAT	5.33	170	170, 128, 86
CAAT	4.82	146	146, 110, 104, 79, 68, 62
OEAT	4.58	156	156, 128, 114, 96, 86, 71

Remark: All the data were resulted from this study. Abbreviation of the compounds listed in "nomenclature" section.

The retention time, precursor ($M + H^+$), and MS/MS spectrum ions are listed in Table 1. It should be noted that all of the reported CMIT data in this study were originally from the results of met-CMIT, where the CMIT was transferred into met-CMIT during the quenching by methanol [13]. Degradations of the ATZ's intermediates were conducted by the stocks from purchase in the separating tests.

3. Results and discussion

3.1. Kinetic model

In a previous work, the decay of ATZ at various $[Fe^{II}]$ and $[H_2O_2]$ concentrations in the combinations of different F/H ratios ($[Fe^{II}]$ to $[H_2O_2]$ ratios) was studied (Chan and Chu, 2003). The reactions of 0.01 mmol L^{-1} ATZ under fixed doses of $[Fe^{II}]$ at 0.20, 0.15, 0.10 and 0.05 mmol L^{-1} with F/H ratios ranging from 3.00 to 0.33 are shown in Fig. 1. Depending on the initial doses and F/H ratios, about 40–98% of ATZ

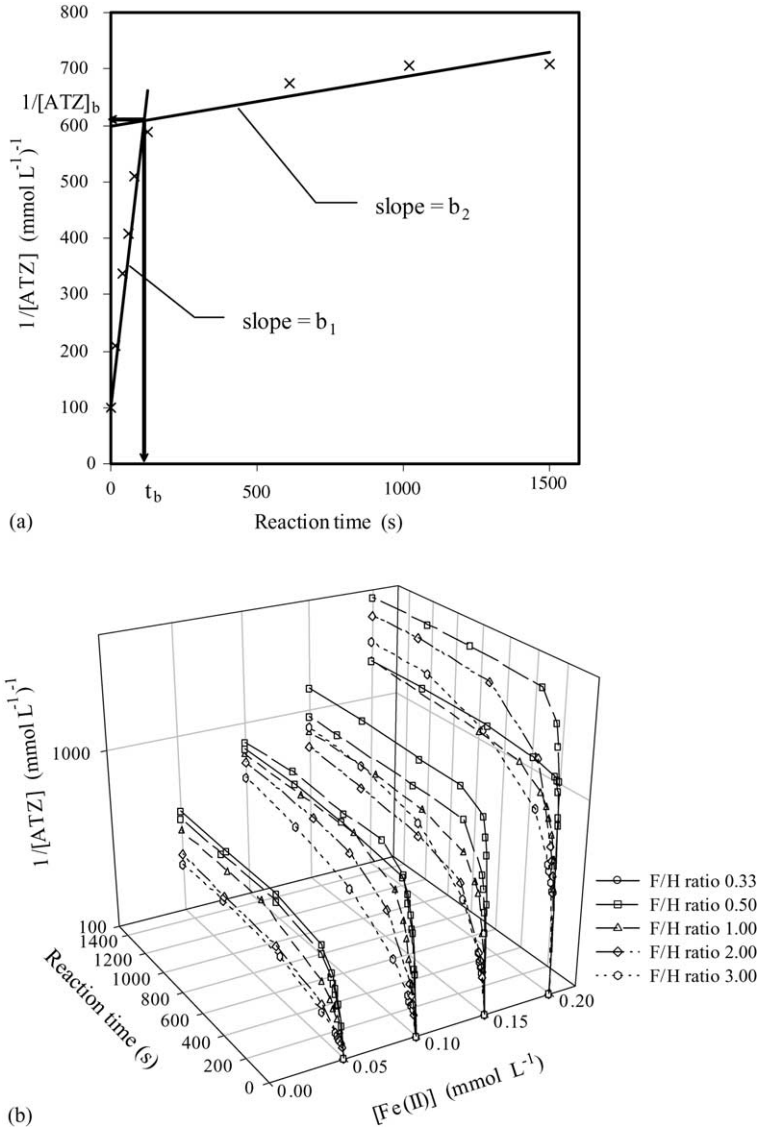

Fig. 1. (a) A typical decay curve of ATZ in a two-stage model for the Fenton's process with 0.10 mmol L^{-1} [Fe^{II}] at F/H ratio of 0.33. The initial $[ATZ]_0$ was 0.01 mmol L^{-1}. (b) The degradation kinetics of ATZ in Fenton's process. F/H ratio is the ratio of [Fe^{II}]-to-[H_2O_2].

was eventually removed at an extended reaction time, indicating that both the Fe^{II} and H_2O_2 were consumable and/or would be deactivated in the process. At a fixed [Fe^{II}] concentration, generally the higher the [H_2O_2] (or the lower the F/H ratio), the faster the ATZ degrade. Likewise, at a fixed F/H ratio, the higher the [Fe^{II}], the faster and higher the fraction of the ATZ degradation. The results suggest that the level of remaining ATZ and rate of ATZ decay depend on the sufficiency of oxidant H_2O_2 and Fe^{II}.

The degradation of ATZ by Fenton's process was a complicated process due to the involvement of many uncountable side reactions and intermediates. The process could not be easily depicted by a simple reaction kinetics, so a new approach was adopted to divide the process into two phases (i.e., a rapid phase I followed by a retarded phase II) for the highest precision. In considering the probe (i.e., ATZ) decay, the reaction kinetics in each phase could be expressed as:

$$\frac{d[ATZ]}{dt} = -k[ATZ]^n \quad (1)$$

where [ATZ] is the concentration of ATZ (mmol L^{-1}) and n is the kinetic order. By using the integral method with least square approach [14], the second-order kinetic was found best fitted with our data (see Table 2). Thus, a two-stage model (in terms of phases I and II) was acquired to describe the process. The two kinetic rate constants therefore were obtained by the following two equations:

$$\text{Phase I}: \quad \frac{1}{[ATZ]} = \frac{1}{[ATZ]_0} + b_1 t \quad (0 \le t \le t_b) \quad (2)$$

$$\text{Phase II}: \quad \frac{1}{[ATZ]} = \frac{1}{[ATZ]_b} + b_2(t - t_b) \quad (t > t_b) \quad (3)$$

Table 2
Determination of the parameters (b_1, b_2, and t_b) of the proposed two-stage model of the degradation of ATZ

$[Fe^{II}]$ (mmol L^{-1})	F/H ratio	Phase I		Phase II		
		b_1 (mmol L^{-1} s^{-1})	R^2	b_2 (mmol L^{-1} s^{-1})	R^2	t_b (s)
0.20	3.00	3.000	0.850	0.750	0.827	279.7
0.20	2.00	7.931	0.984	0.302	0.845	270.0
0.20	1.00	8.910	0.896	0.284	0.990	124.7
0.20	0.50	21.445	0.717	0.224	0.841	94.1
0.20	0.33	24.090	0.913	0.126	0.809	56.9
0.15	3.00	1.341	0.962	0.215	0.928	300.0
0.15	2.00	3.211	0.966	0.122	0.885	283.9
0.15	1.00	5.305	0.985	0.074	0.650	166.0
0.15	0.50	7.657	0.997	0.037	0.979	101.8
0.15	0.33	14.400	0.958	0.033	0.963	75.0
0.10	3.00	0.667	0.887	0.083	0.995	360.0
0.10	2.00	1.103	0.974	0.033	0.959	348.2
0.10	1.00	2.151	0.990	0.031	0.875	297.9
0.10	0.50	4.350	0.992	0.021	0.157	205.3
0.10	0.33	4.452	0.915	0.010	0.755	178.9
0.05	3.00	0.268	0.526	0.017	0.751	253.4
0.05	2.00	0.325	0.802	0.024	0.939	251.8
0.05	1.00	0.750	0.944	0.011	0.052	247.4
0.05	0.50	1.355	0.974	0.007	0.802	174.6
0.05	0.33	1.675	0.969	0.005	0.956	160.7

Since the $[ATZ]_b$ can be solved from Eq. (2) when t is t_b:

$$\frac{1}{[ATZ]_b} = \frac{1}{[ATZ]_0} + b_1 t_b \quad (4)$$

The overall equation in phase II is available by merging Eqs. (3) and (4):

$$\frac{1}{[ATZ]} = \frac{1}{[ATZ]_0} + b_1 t_b + b_2(t - t_b) \quad (t > t_b) \quad (5)$$

where $[ATZ]_0$ and $[ATZ]_b$ are the concentrations of ATZ (mmol L^{-1}) at the beginning and at the break point of the two phases, respectively. The break point time, t_b, in second, is the observed time separating phases I and II in the reaction. The b_1 and b_2 are the rate constants (mmol L^{-1} s^{-1}) of phases I and II, and the schematic diagram of a typical two-stage kinetic is plotted in Fig. 1. The parameters b_1, b_2 and t_b were determined and listed in Table 2. Thus, the first correlation that can be identified is the relationships between b_2 and b_1, as plotted in Fig. 2.

Four parallel straight lines were obtained from the four different ferrous concentrations at 0.20, 0.15, 0.10 and 0.05 mmol L^{-1}, if logarithmic axes were used. The linearized curves with a common slope of −0.682 were determined and formulated by Eq. (6):

$$\ln b_2 = I_b - 0.682 \ln b_1 \quad (6)$$

where I_b is the intercept of all regression lines in Fig. 2. These relationships show that the reaction kinetics of phases I and II were inter-correlated. It shows that the increment of $[Fe^{II}]$ will increase both b_1 and b_2, justifying that a higher concentration of ferrous ions results in higher oxidative power of Fenton's process. If the initial reagent concentration is high, the corresponding remaining of these reagents should also be higher in the phase II, which makes the b_1 and b_2 a positive correlation. The negative slope indicates that the b_1 and b_2 do not have a proportional relationship; instead, an increase of b_1 will reduce b_2 accordingly in an exponential trend, and vice versa. This is an interesting observation which may be rationalized by the availability of ATZ in the system. As the oxidative power of Fenton's process was low and can only degrade ATZ partially in phase I (lower b_1), more $[ATZ]_b$ would be available in the solution for the phase II reaction. Thus higher initial $[ATZ]_b$ concentration resulted in faster decay (higher b_2). Conversely, as the oxidative power of Fenton's process was high, most of the ATZ was degraded in phase I (higher b_1), and very low $[ATZ]_b$ was left for the

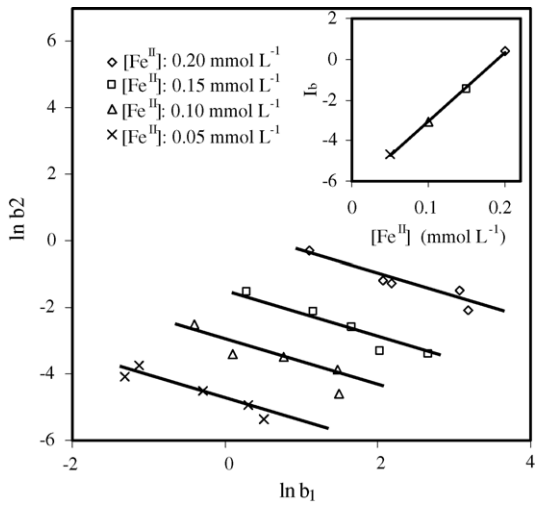

Fig. 2. Correlation of the rate constants b_1 and b_2 of phases I and II kinetics (insert: correlation of I_b and ferrous concentrations $[Fe^{II}]$).

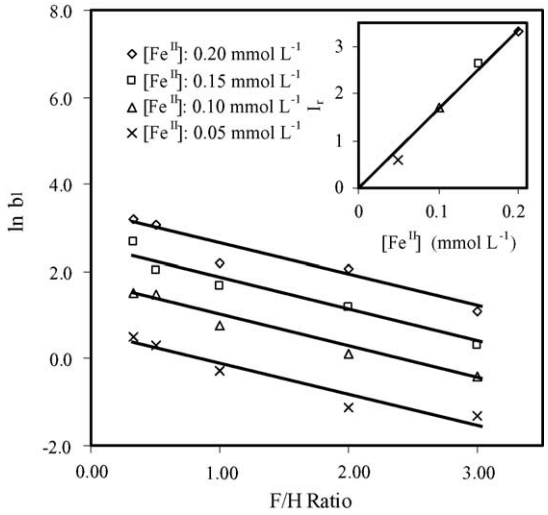

Fig. 3. Correlation of the phase I rate constant b_1 and F/H ratio (insert: correlation of I_r and ferrous concentrations [Fe^{II}]).

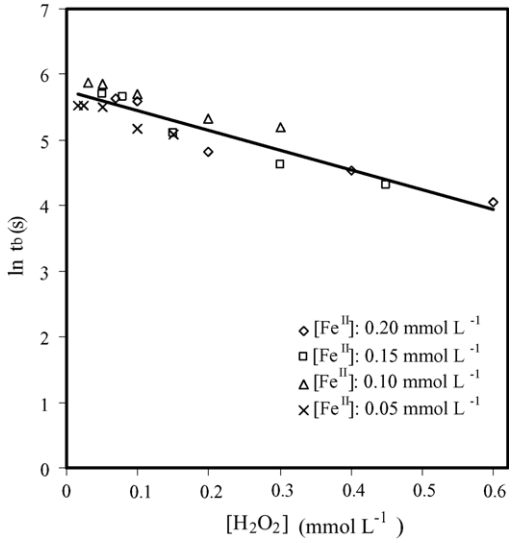

Fig. 4. Correlation on the break point time, t_b, and hydrogen peroxide dosage, [H_2O_2].

phase II reaction, thus resulting in a lower b_2. The intercepts I_b were clearly dependent on ferrous concentrations with an r^2 of 0.999 (see the insert in Fig. 2), the linear equation is therefore:

$$I_b = 34.048[\text{Fe(II)}] - 6.452 \quad (7)$$

in which [Fe^{II}] (in mmol L^{-1}) is the ferrous concentration used in the system.

The phase I decay rate constant b_1 can also be resolved and correlated with the F/H ratio as depicted in Fig. 3; similarly, four parallel lines with a negative common slope of 0.818 was formulated in Eq. (8):

$$\ln b_1 = I_r - 0.818\frac{[\text{Fe(II)}]}{[H_2O_2]} \quad (8)$$

where [H_2O_2] (in mmol L^{-1}) is the hydrogen peroxide used in the system, and I_r is the intercept, which can be correlated to ferrous concentrations with an r^2 of 0.981 (see the insert in Fig. 3). The linear equation is therefore:

$$I_r = 16.738[\text{Fe(II)}] \quad (9)$$

After the b_1 and I_b were worked out, the phase II decay rate b_2 could easily be resolved by Eq. (6).

The break point time, t_b (s) was used to distinguish phases I and II in the reaction. Fig. 4 shows that the break point time can be co-related with [H_2O_2] by Eq. (10):

$$\ln t_b = 5.759 - 3.029[H_2O_2] \quad (10)$$

The physical meaning of Eq. (10) is that the system will take a longer time to reach break point (or terminate phase I) if less hydrogen peroxide is used. This is likely due to the lack of oxidant source in the solution, which will reduce the chance of molecular collisions between the reactants in the sub-reactions [12]. Therefore, more time will be required to accomplish phase I.

3.2. Application of the model

For general practices, it is better to re-organize the above equations by using some terms that are ready to use, such as [Fe^{II}] and [H_2O_2]. Therefore, the equations regarding b_1, b_2, and t_b are rewritten in Eqs. (11)–(13) as follows:

$$b_1 = \exp\left(16.738[\text{Fe(II)}] - 0.818\frac{[\text{Fe(II)}]}{[H_2O_2]}\right) \quad (11)$$

$$b_2 = \exp\left(22.633[\text{Fe(II)}] + 0.558\frac{[\text{Fe(II)}]}{[H_2O_2]} - 6.452\right) \quad (12)$$

$$t_b = \exp(5.759 - 3.029[H_2O_2]) \quad (13)$$

Combining Eqs. (2), (5), (11)–(13) completes the kinetic model, in which the remaining ATZ in the presence of Fenton's reagent at any practical combination and reaction time becomes predictable. The predicted curves based on the proposed model were compared to the raw data and a typical example is depicted in Fig. 5. The observed error was less than 8%, which justifies that the proposed model can predict the ATZ decay successfully.

To fully expand the usefulness of the proposed model, Fig. 6 was custom-made based on the proposed model. It shows the performance of ATZ decay (%) under different combinations of ferrous ion and hydrogen peroxide and their associated rate constants in phase I, b_1. The reason for using the phase I reaction as the performance indicator is because the majority of the ATZ is degraded in phase I, so that the inefficient and prolonged phase II reaction is not appropriate and will not be accounted for in the system design. In addition, it is interesting to find out that in order to achieve the same ATZ decay performance, the possible combination of Fe^{II} and H_2O_2 is not limited to one. Such characteristics make the Fenton' process very complex to design properly; therefore, a

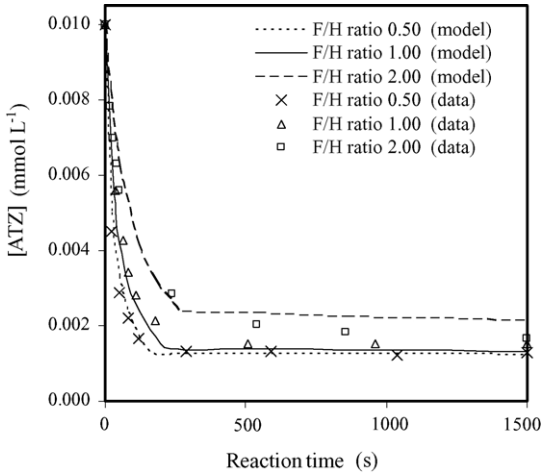

Fig. 5. Prediction of ATZ oxidation by the proposed model in Fenton's process with 0.10 mmol L^{-1} of [Fe^{II}] in various F/H ratios.

procedure to optimize the treatment plant design of Fenton's system is proposed:

(i) Draw a horizontal line in Fig. 6 to identify the required effluent quality at the end of phase I. This will return many combinations of Fe^{II} and H_2O_2 that will allow the designers to achieve similar effluent quality for direct discharge, and the chemical cost of each combination should be evaluated.

(ii) The phase I decay rates (b_1) for those selected Fe^{II} and H_2O_2 combinations that resulted from part (i) can be identified from the *x*-axis of Fig. 6, since the reactor size can be determined by the retention time (under a constant flow rate of course), and the retention time can be solved from the identified decay rate b_1. The capital cost of all selected Fenton's reagent combinations can therefore be calculated.

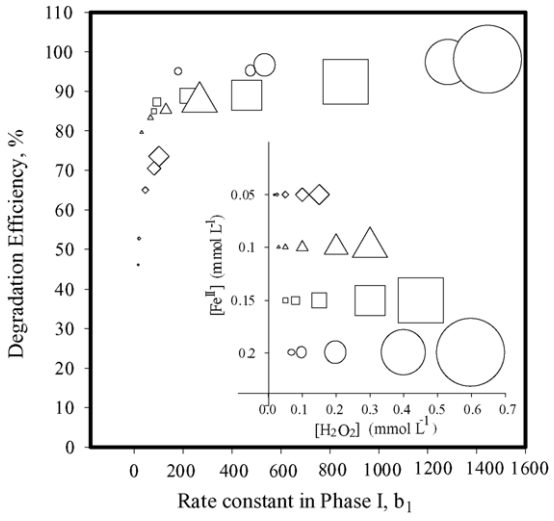

Fig. 6. Performances of Fenton's process for ATZ decay at the end of phase I.

(iii) The Fenton's reagent combination that gives the minimal sum of the chemical and capital costs from the above two criteria should be adopted for design.

Therefore, based on the proposed model and Fig. 6, the optimization of the Fenton's process and treatment plant design is realized.

3.3. Atrazine degradation mechanism

In this study, ATZ was degraded by 0.1 mmol L^{-1}[Fe^{II}] and [H_2O_2] and 10 intermediates were identified during the Fenton's process. The transformation/degradation pathways were organized and shown in Fig. 7. The intermediates were categorized into primary, secondary and tertiary intermediates, and all of them were sorted by chlorinated or dechlorinated products. In the process, the major oxidant was the $HO^{\bullet}$, since $HOO^{\bullet}$ and its conjugate base $O_2^{\bullet}$ were much less reactive as hydroxyl radicals [15,16]. The presence of $HO^{\bullet}$ initiated the decay of ATZ through alkylic-oxidation (alkylamino side-chain oxidation), dealkylation (alkylic side-chain cleavage), and/or dechlorination (hydroxylation at the chlorine site), and generated the corresponding intermediates. Dealkylation might be occurred by the abstraction of hydrogen atom (H) from the secondary carbon atom (C) of the ethylamino side-chain producing a free radical (Eq. (14)) [10], which subsequently produced various intermediates.

$$HO^{\bullet} + RNHCH_2CH_3\,(\equiv ATZ) \rightarrow H_2O + RNHC^{\bullet}HCH_3 \quad (14)$$

Dechlorination–hydroxylation could be initiated by an $HO^{\bullet}$ attack of the *s*-triazine ring at the C–Cl position, resulting in an oxidation of the aromatic heterocyclic ring (of ATZ), while hydroxylation occurred simultaneously, so that the chlorine atom was substituted by a hydroxyl group. Hence, various hydroxylated *s*-triazines formed in the solution.

Previously, the Fenton's process was characterized as a process with a rapid initial reaction rate, followed by a stagnant stage in an extended reaction time (after 700 s in this case) due to the rapid initial production and consumption of oxidative reagents, respectively. The short-lived property and unselective reactivity of $HO^{\bullet}$ might limit the extent of the removal of ATZ and even lower the reduction of other intermediates. However, the further degradation of the concentrations of derivatives in the stagnant stage was observed (after 700 s). This could result from some less reactive radicals such as $HOO^{\bullet}$, $R^{\bullet}$, $ROO^{\bullet}$, which were generated during Fenton's process, and/or the transient oxygen species that resulted from residual H_2O_2 [17]. However, these radicals were not active enough to oxidize ATZ, but were still useful in oxidizing selective intermediates in the solution.

In Fig. 8, the rise of concentrations of three primary intermediates CDET, CMIT, and CDIT (8, 35 and 53%, respectively, at 350 s reaction time) (except OIET) in the beginning of reaction suggested that the decay of ATZ was

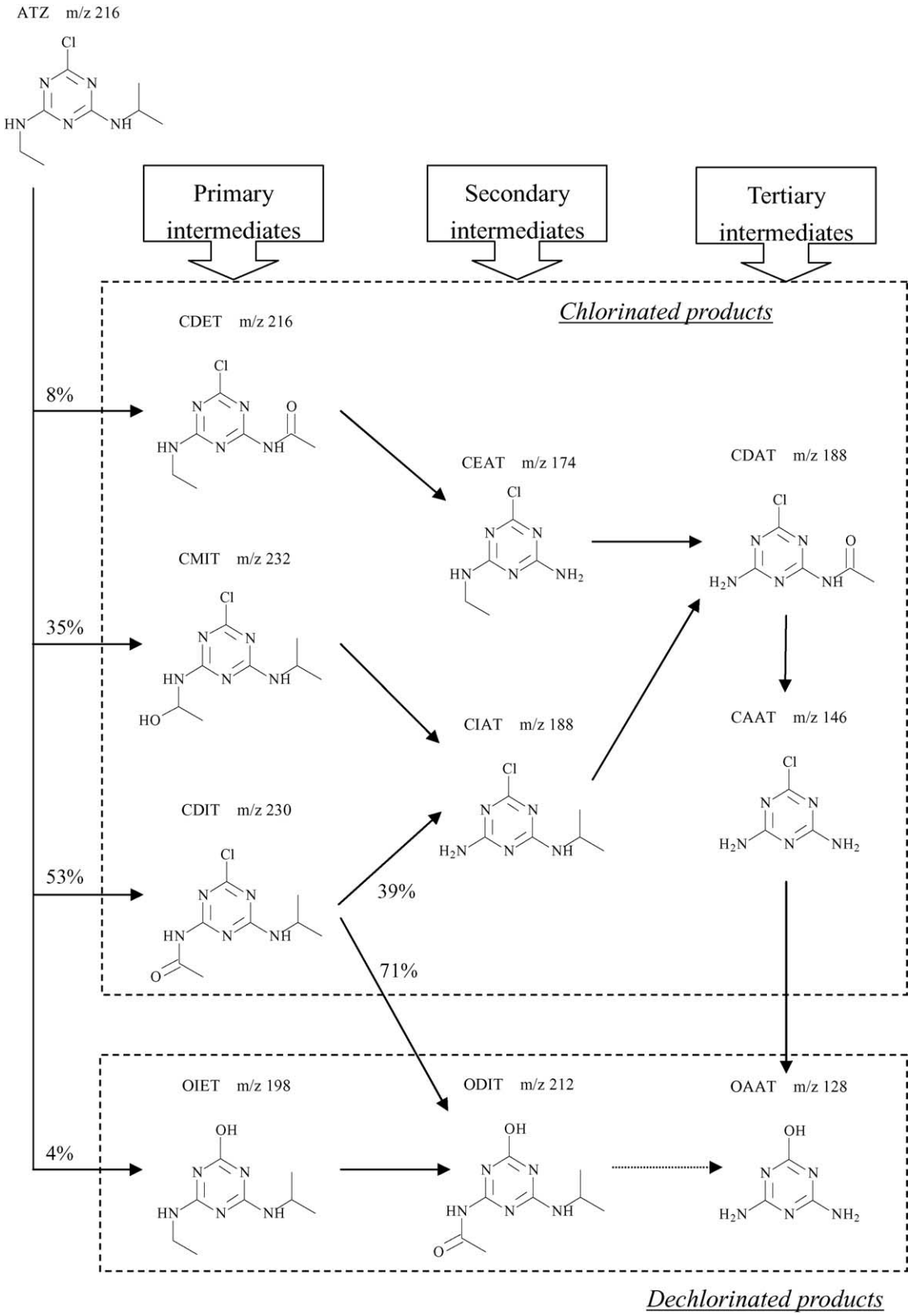

Fig. 7. Degradation pathways of ATZ. Percentages (at 350 s reaction time) given for the relative importance of a pathway (no indications mean 100%).

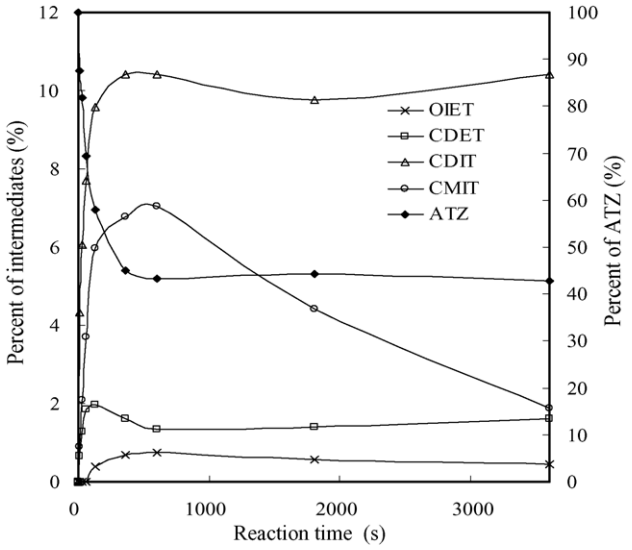

Fig. 8. Degradation profile of ATZ to the primary intermediates (i.e., OIET, CDET, CDIT and CMIT).

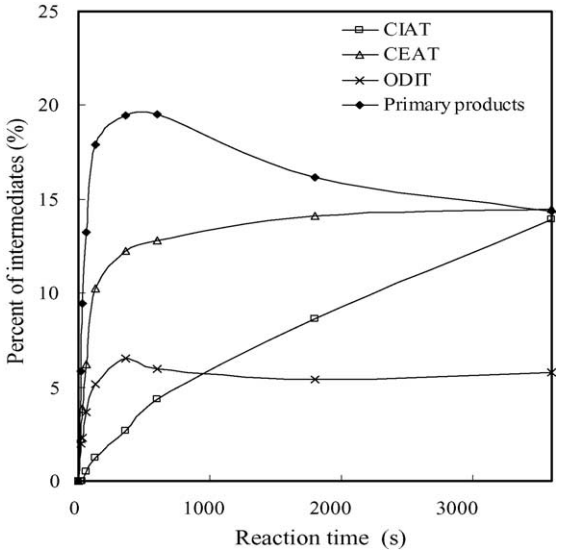

Fig. 9. Degradation profile of the primary intermediates to the secondary intermediates (i.e., CIAT, CEAT and ODIT).

mainly initiated by alkylic-oxidation. Then, the dealkylation of CDET yielded CEAT at a high concentration, followed by another alkylic-oxidation to form CDAT in the next 200 s (Figs. 7 and 9). The comparatively high [CEAT] might result from the higher dealkylation rate of CDET (i.e., the formation of CEAT) than that of the decay of CEAT. A similar reaction was also observed on CDIT and CMIT. Thus, a dealkylated product of CIAT gradually increased after the [CDIT] and [CMIT] descended from their peaks of concentration. By conducting a separated test on the degradation of CIAT (CIAT as the starting probe), this showed that CIAT subsequently formed CDAT by alkylic-oxidation. It is interesting to point out that [CIAT] rose continuously in the stagnant stage, while the $HO^{\bullet}$ was known to be deficient. This is likely due to the presence of less reactive radicals ($HOO^{\bullet}$ and $O_2^{\bullet}$) in the solutions, which were in favor of reacting with the methylethanolamino structure of CMIT [13]. Therefore, the CMIT could be easily degraded to CIAT by weaker oxidants.

On the other hand, the dechlorinated product OIET was observed at a lower concentration with a lower transformation rate (only 4% at 360 s reaction time) (Fig. 8). This suggested that the dechlorination of ATZ by Fenton's process was not a preferential pathway while competing with alkylic-oxidation and the dealkylation of ATZ. In a separate test involving the degradation of OIET as the starting probe by Fenton's process, the alkylic-oxidation product, ODIT, was found to be the sole degradation intermediate of OIET (Fig. 7). According to Fig. 9, however, ODIT was detected before the formation of OIET, suggesting that the oxidation of OIET was not the only source responsible for the formation of ODIT during the degradation of ATZ. Apparently, the dechlorination–hydroxylation of CDIT (71% of total) was the additional pathway in generating ODIT.

The degradation profiles of the primary, secondary and tertiary intermediates were depicted in Fig. 10. The CDAT was further dealkylated to the CAAT that exhibited a sharp/major peak compared to the others. The high concentration of CAAT justified that, again, dealkylation is the dominant pathway in Fenton's process. After the [ODIT] and [CAAT] dropped from their peak concentration, [OAAT] reached its maximum. This could be the result of both the dealkylation of ODIT and the dechlorination–hydroxylation of CAAT. Judging from the structure of OAAT, no side-chain or functional group could be further oxidized easily without opening the aromatic heterocyclic ring or replacing the amine groups. It suggested that OAAT was the terminal product of ATZ decay in Fenton's process.

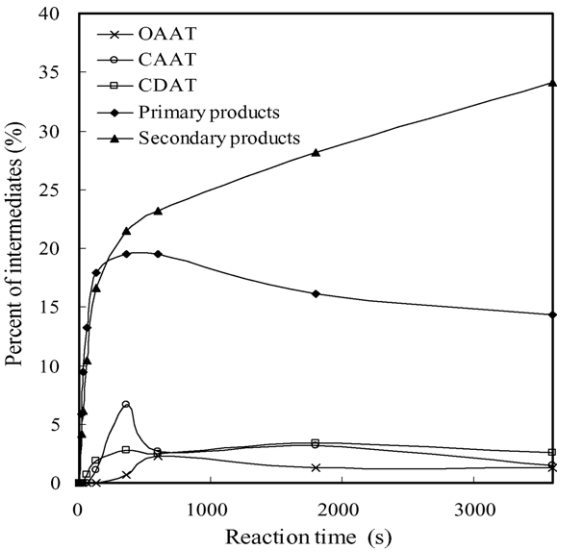

Fig. 10. Degradation profile of the primary intermediates and secondary intermediates to OAAT, CAAT and CDAT.

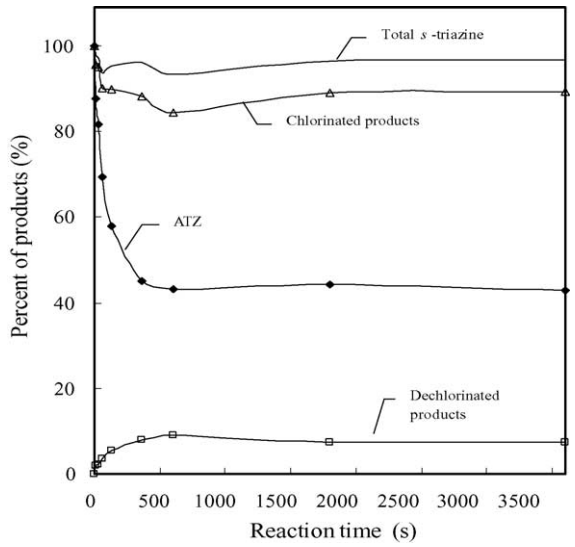

Fig. 11. Comparison of chlorinated and dechlorinated products of the degradation of ATZ by Fenton's process.

The transformation of ATZ, its intermediates (in terms of chlorinated and dechlorinated products), and the mass balance (in *s*-triazine) in Fenton's process were incorporated in Fig. 11. According to the figure, the process slowed down after 700 s and the ATZ remained at 42%. The chlorinated products (including ATZ) decreased but remained at high level through out the process. On the other hand, the dechlorinated products increased accordingly. Due to the depletion of oxidants, the dechlorinated products were detected at low levels of concentration (<10% in total). Judging from Figs. 9–11, the formation of dechlorinated intermediates was mainly observed after the decay of chlorinated intermediates and the concentration of the latter is maintained at low level; it was suggested that the products that have been chlorinated through alkylic-oxidation and/or dealkylation were the dominant species in Fenton's process. This result has excluded the possibility of the fast decay of dechlorinated tertiary intermediates, because the mass balance of *s*-triazine (93% throughout the process) indicated that most of the residuals in the solution were close to a stagnant state. In addition, the high *s*-triazine fraction suggested that no ring cleavage occurred in Fenton's process.

4. Conclusions

The use of ferrous ion and hydrogen peroxide is an effective treatment process for oxidizing toxic compounds that are not biodegradable in conventional treatments. In earlier studies, the performance of Fenton's process was presented in many diverse ways, and made it difficult to make comparison and draw conclusions. Therefore, the main drawbacks of this process are its complexities and the difficulties of producing an efficient and proper engineering design. In this study, by investigating the reaction kinetics under different reaction conditions of Fenton's process, a practical model for predicting ATZ decay performance based on two simple parameters [Fe^{II}] and [H_2O_2] was derived successfully. The proposed model was further expanded through the re-combination of the Fe^{II} and H_2O_2 dosages, compound decay performance, and decay rates, so that the optimization of treatment performance and treatment plant design is possible.

Besides, the transformation mechanism of ATZ degradation by Fenton's process was successfully investigated. Totally 10 intermediates were identified. The degradation pathways of ATZ were evaluated. It was found that the alkylic-oxidation followed by dealkylation and dechlorination–hydroxylation were likely the major pathways. Besides, there was no ring-cleavage occurred on the ATZ.

Acknowledgement

The work described in this paper was supported by a grant from the University Research Fund of the Hong Kong Polytechnic University (GV-952).

References

[1] R.R. Trussell, Endocrine disruptors and the water industry, J. Am. Water Works Assoc. 93 (2001) 58–65.
[2] Ciba-Geigy Corporation, Environmental Fate Reference Data Source Book for Atrazine, Greensboro, NC, USA, 1994.
[3] G.W. Stratton, Effects of the herbicide atrazine and its degradation products, alone and in combination, on phototrophic microorganisms, Arch. Environ. Contam. Toxicol. 13 (1984) 35–42.
[4] R. Eisler, Atrazine hazards to fish, wildlife and invertebrates: a synoptic review: US, Fish Wildl. Serv. Biol. Rep. 85 (1989) 1–18.
[5] G. Rupert, R. Bauer, G.J. Heisler, The photo-Fenton reaction. An effective photochemical wastewater treatment process, Photochem. Photobiol. A: Chem. 73 (1993) 75–78.
[6] D.L. Sedlak, A.W. Andern, Oxidation of chlorobenzene with Fenton's reagent, Environ. Sci. Technol. 25 (1991) 777–782.
[7] M.E. Lindsey, M.A. Tarr, Quantitation of hydroxyl radical during Fenton's oxidation following a single addition of iron and peroxide, Chemosphere 41 (2000) 409–417.
[8] R.J. Watts, B.C. Bottenberg, T.F. Hess, M.D. Gensen, A.L. Teel, Role of reductants in the enhanced desorption and transformation of chloroalophatic compounds by modified Fenton's reactions, Environ. Sci. Technol. 33 (1999) 3432–3437.
[9] B.K. Aldershof, R.M. Dennis, C.J. Kunitsky, Study of the decomposition of four commercially available hydrogen peroxide solutions by Fenton's reagent, Water Environ. Res. 69 (1997) 1052–1056.
[10] S.M. Arnold, W.J. Hickey, R.F. Harris, Degradation of atrazine by Fenton's reagent: condition optimization and product quantification, Environ. Sci. Technol. 29 (1995) 2083–2089.
[11] J.R. Plimmer, P.C. Kearney, U.I. Klingebiel, *s*-Triazine herbicide dealkylation by free-radical generating systems, J. Agric. Food Chem. 19 (1971) 572–573.
[12] K.H. Chan, W. Chu, Modeling the reaction kinetics of Fenton's process on the removal of atrazine, Chemosphere 51 (2003) 305–311.
[13] S. Nélieu, L. Kerhoas, J. Einhorn, Degradation of atrazine into ammeline by combined ozone/hydrogen peroxide treatment in water, Environ. Sci. Technol. 34 (2000) 430–437.

[14] S.T. Chapra, Surface Water-Quality Modeling, McGraw-Hill, New York, 1997, pp. 24–36.
[15] B.H.J. Bielski, D.E. Cabelli, R.L. Arudi, Reactivity of H_2O_2/O_2-radicals in aqueous solution, J. Phys. Chem.: Ref. Data 14 (1985) 1041–1100.
[16] A.A. Frimer, in: M.G. Simiuc, et al. (Eds.), Oxygen Radicals in Biology and Medicine, Plenum Press, New York, 1988, pp. 29–38.
[17] L.M. Dorfman, G.E. Adams, Reactivity of the hydroxyl radical in aqueous solutions, Report No. NSRDS-NBS-46, National Bureau of Standards, Washington, DC, 1973, pp. 22–31.